

Buckling analysis of a sandwich plate with polymeric core integrated with piezo-electro-magnetic layers reinforced by graphene platelets

Pooya Nikbakhsh and Mehdi Mohammadimehr*

Department of Solid Mechanics, Faculty of Mechanical Engineering, University of Kashan, Kashan, Iran

(Received September 12, 2021, Revised January 8, 2022, Accepted January 20, 2022)

Abstract. In the present work, we proposed an analytical study on buckling behavior of a sandwich plate with polymeric core integrated with piezo-electro-magnetic layers such as BaTiO₃ and CoFe₂O₄ reinforced by graphene platelets (GPLs). The Halpin-Tsai micromechanics model is used to describe the properties of the polymeric core. The governing equations of equilibrium are obtained from first-order shear deformation theory (FSDT) and the Navier's method is employed to solve the equations. The results show the effect of different parameters such as thickness, length, weight fraction of GPLs, and also effect of electric and magnetic field on critical buckling load. The result of this study can be obtained in the aerospace industry and also in the design of sensors and actuators.

Keywords: buckling analysis; FSDT; graphene platelets; Halpin-Tsai model; piezo-electro-magnetic face sheets; polymeric core; sandwich plate

1. Introduction

Sandwich constructions are one of the most used composite structures that widely employed in different industries such as aerospace, automotive, shipbuilding. Generally, a sandwich structure made of two facesheets and low strength and weight core like foam, honeycomb and that leads to overall low weight and high strength and stiffness. Carbon nanotubes have been discovered in 1991 and used as reinforcements in most engineering fields due to high mechanical, thermal and magnetic properties (Jia *et al.* 2011, Sun *et al.* 2005, Yang *et al.* 2018).

Mohammadimehr *et al.* (2017) conducted analytical study on nonlinear free vibration of functionally garded carbon nanotubes (CNT) reinforced composite sandwich and achieve optimum thickness ratio for the highest stiffness. Karimiasl *et al.* (2020) studied nonlinear vibration analysis of multiscale doubly curved sandwich nanoshell and developed a smart model of sandwich composite nanoshell based on strain gradient-nonlocal theory. Ghorbanpour Arani *et al.* (2011) investigated the buckling behavior of composite plate reinforced by single-walled carbon nanotubes (SWCNTs) under uniaxial compressive load by using finite element and showed that agglomeration of carbon nanotubes (CNTs) have significant influence on the buckling load and properties of CNT reinforced composite. Arefi *et al.* (2019) considered the bending response of functionally graded

*Corresponding author, Professor, E-mail: mmohammadimehr@kashanu.ac.ir

(FG) graphene nanoplatelets reinforced curved nanobeams resting on a Pasternak foundation based on the first-order shear deformation theory (FSDT). Mousavi *et al.* (2019) studied the buckling behavior of hollow circular sandwich plate with porosity in core and FG-CNT piezoelectric facesheets. Using Reddy's third-order shear deformation shell theory, Duc (2016) analyzed nonlinear thermal dynamic of eccentrically stiffened S-FGM circular cylindrical shells surrounded on elastic foundations. The structure is affected by mechanical, damping loads and temperature and the Bubnov-Galerkin method is applied to acquire results. He concluded that temperature, elastic foundations, and outside stiffeners had a significant impact on dynamic response of the S-FGM circular cylindrical shells. Over another study which conducted by this author in the same year on nonlinear thermo- electro-mechanical dynamic response of a functionally graded sandwich circular cylindrical shells, he explored the impact of material properties, imperfection, and thermo-electro-mechanical and damping loads on the nonlinear dynamic response of the shells. Also, an excellent investigations have been carried out on nonlinear static, buckling and postbuckling analysis of shells and panels (Vuong and Duc 2020, Duc and Tung 2010, Khoa *et al.* 2017). They employed Galerkin method and the fourth-order Runge-Kutta method to derive the results which the outcome depicts the effect of material properties, imperfection, and thermo-electro-mechanical and damping loads on the nonlinear dynamic response of the shells.

Graphene nanoplatelets (GPLs) are newly used 2D nanofillers that have recently investigated and take much attention. As a comparison with CNTs, it has much stronger bonding due to their more surface area. Also, reinforcements such as carbon nanotubes and graphene platelets in polymer-based nanocomposites leads to enhance in mechanical properties in which these properties for align nanotubes is better than randomly oriented (2019). By using Navier's type solution based on FSDT, Song *et al.* (2017, 2018, 2017) researched the influence of different GPLs parameters on bending, buckling, free and forced vibration of FG graphene reinforced polymer plates. García-Macías *et al.* (2018) by analyzing the bending and free vibration behaviors of FG plates reinforced by graphene platelets (GPLs) and CNTs by considering η determined that stiffing effect of GPLs in compare with CNTs is more. Yang *et al.* (2020) illustrated a parametric study on dynamic buckling of FG-GPL reinforced composite shallow arches under a central point force. Wang *et al.* (2019) investigated buckling and post-buckling of composite beam reinforced with GPLs by consideration dielectric properties. Barati *et al.* (2020) researched on forced vibration characteristic of thermally loaded nanocomposite reinforced by GPLs. Thai *et al.* (2019) obtained numerical method based on refined plate theory for analyzing FG-GPL reinforced composite structure. Li *et al.* (2019) presented the load bearing capacity of the confined (Functionally graded porous) FGP-GPL arch under a thermal rise field. Thai *et al.* (2019) proposed a size dependent model to free vibration analysis of multilayer FG-GPL reinforced composite microplate. Pashmforoush *et al.* (2019) investigated vibration and statically analysis on FG-graphene reinforced composite plate based on high-order shear deformation theory (HSST).

Some researchers worked about piezo-electro-magnetic fields in face sheets that will produce voltages by deformation in sandwich structures as follows

Mohammadimehr *et al.* (2016) presented electro-elastic analysis of a sandwich thick plate considering FG core and composite piezoelectric layers on Pasternak foundation using third-order shear deformation theory (TSDT). Chan *et al.* (2020) has employed Hamilton's principle to derive the motion equations of a piezoelectric functionally graded porous truncated conical panel, and analyzed the results by Galerkin's and Runge-Kutta methods. In their study, the effect of porosity distribution, porosity coefficient, applied actuator voltage and temperature has been investigated on nonlinear dynamic response and free vibration of functionally graded porous (FGP) panel. The

outcome shows the porosity distribution and coefficient have effect on the natural frequencies and deflection amplitudes of the piezoelectric FGP pan, and by elevating the temperature, the deflection will increase as well.

Selim *et al.* (2019) considered GPLs reinforced composite with piezoelectric facesheets effect on mechanical properties as they performed control by active vibration. Mohammadimehr and shahedi (2016) investigated the nonlinear free vibration of magneto-electro-mechanical sandwich beam with varying FG dispersion on Pasternak foundation. Mao *et al.* (2019) examined FG-GPLs reinforced Poly vinylidene Fluoride (PVDF) matrix by different distribution modes. Zhao *et al.* (2020) developed dynamic stability by the effect of porosity characteristics on FG arch reinforced by GPLs. Ghadiri *et al.* (2019) studied sandwich structure with piezoelectric core integrated with graphene nanoplate facesheets and proposed the effect of voltage and pulse force on nonlinear frequency. GhorbanpourArani *et al.* (2019) studied pull-in instability of a sandwich structure with reinforced polymeric core and piezoelectric face sheets under electro-magneto-mechanical loadings. Bamdad *et al.* (2019) analyzed buckling and vibration behavior of magneto-electro-elastic sandwich beam with different porous distribution in core and CNT dispersions in facesheets. Taherifar *et al.* (2019) presented buckling analyses of composite concrete plate reinforced by piezoelectric nanoparticles based on Halpin-Tsai model to obtain the effective material properties of nano composite concrete plate and third order shear deformation theory. Rajabi and Mohammadimehr (2019) considered bending analysis of a micro sandwich skew plate with isotropic core and piezoelectric composite face sheets reinforced by carbon nanotube on elastic foundations. Rahi *et al.* (2021) presented a simplified numerical method for nonlocal static and dynamic analysis of a graphene nanoplate. Canbay *et al.* (2021) studied thermostructural shape memory effect observations of ductile Cu-Al-Mn smart alloy. Rabia *et al.* (2020) considered predictions of the maximum plate end stresses of imperfect FRP strengthened RC beams: study and analysis. Namayandeh *et al.* (2020) studied temperature and thermal stress distributions in a hollow circular cylinder composed of anisotropic and isotropic materials. Hadji and Bernard (2020) investigated bending and free vibration analysis of functionally graded beams on elastic foundations with analytical validation. Vibration analysis has brought a special charm for many researchers around the world due to their vital role in condition monitoring of various types of mechanical structures. In the recent years, a large number of scientists investigated both linear and nonlinear vibration response on sandwich plates and shells (Duc *et al.* 2016, Cong and Duc 2016, Duc and Tung 2010, Duc *et al.* 2021). Quan *et al.* (2021) and Dat *et al.* (2020) studied an analytical method for nonlinear thermo-electro-magneto vibration of a plates. In their contribution, the influence of elastic foundations, geometrical parameters, temperature and moisture on the nonlinear vibration of the plate are investigated. The results illustrate that elastic foundations has a positive effect and temperature and moisture have a negative influence. Duc *et al.* (2015) presented the nonlinear buckling of higher deformable S-FGM thick circular cylindrical shells with metal-ceramic-metal layers surrounded on elastic foundations in thermal environment. In the other work, Thang *et al.* (2017) illustrated thermomechanical buckling and post-buckling of cylindrical shell with functionally graded coatings and reinforced by stringers. Anitescu *et al.* (2019) and Guo *et al.* (2019) worked about artificial and deep neural networks that are a topic of great interest in the machine and deep learning community due to their ability to solve very difficult problems, respectively. Using a collocation formulation, Anitescu *et al.* (2019) solved second order boundary value problems such as Poisson's equation and Helmholtz equation, also, Guo *et al.* (2019) built a loss function with the aim that the governing partial differential equations (PDEs) of Kirchhoff plate bending problems, and the boundary/initial conditions are minimised at those collocation points. In general, in order to

solve Partial Differential Equations (PDEs) that represent real systems to an acceptable degree, analytical methods are usually not enough. One has to resort to discretization methods. For engineering problems, probably the best-known option is the finite element method (FEM). However, powerful alternatives such as mesh-free methods and Isogeometric Analysis (IGA) are also available. Thus, Samaniego *et al.* (2020) presented an energy approach to the solution of partial differential equations in computational mechanics via machine learning including concepts, implementation and applications. Rabczuk *et al.* (2019) presented a novel nonlocal operator theory based on the variational principle for the solution of partial differential equations. Their present nonlocal formulation allows the assembling of the tangent stiffness matrix with ease and simplicity, which is necessary for the eigenvalue analysis such as the waveguide problem. Yang *et al.* (2020) illustrated an analytical investigation on the nonlinear buckling behavior of graphene platelets reinforced dielectric composite (GPLRDC) arches with rotational end restraints under applied electric and uniform radial load. They estimated the effective materials properties of GPLRDC, including the elastic modulus and dielectric permittivity, by employing effective medium theory (EMT). They investigated the analytical solutions for nonlinear equilibrium, critical load of limit point buckling and bifurcation buckling of the GPLRDC arch are derived according to the principle of virtual work. In the other work, they (2022) considered an analytical study on the asymmetric static and dynamic buckling of a pinned-fixed functionally graded graphene nanoplatelet reinforced composite (FG-GPLRC) arch under thermal conditions. Tam *et al.* (2020) investigated the nonlinear bending behaviours of multilayer functionally graded graphene nanoplatelet-reinforced composite (FG-GPLRC) beams elastically restrained at both ends and with an open edge crack. Yang *et al.* (2021a) presented a dynamic buckling analysis for a rotationally restrained functionally graded (FG) graphene nanoplatelets (GPLs) reinforced composite (FG-GPLRC) porous arch under a uniform step load where GPL nanofillers are uniformly dispersed while the porosity coefficient varies along the thickness direction of the arch. Yang *et al.* (2021b) considered the small scale-dependent geometrical nonlinear flexural response of arbitrary-shaped microplates having variable thickness made of functional graded (FG) composites.

In the present work, the authors have been investigated an analytical study on buckling behavior of a sandwich plate with polymeric core integrated with piezo-electro-magnetic layers such as BaTiO₃ and CoFe₂O₄ reinforced by graphene platelets (GPLs). They used the GPL as reinforcement to increase the stiffness of a sandwich plate. Also, they employed polymeric core to reduce the weight of these structure, because in mechanical science, the researcher follow to

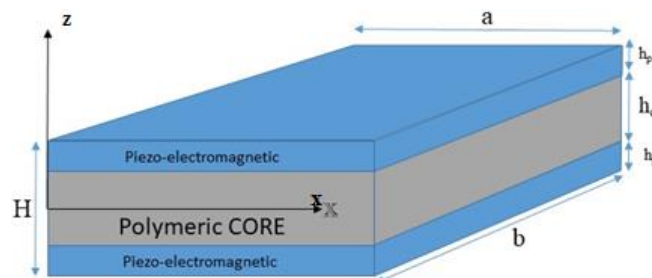


Fig. 1 A schematic view of three-layered sandwich plate with polymeric core and piezo-electro-magnetic face-sheets

increase the high strength to weight. Moreover, the authors considered the piezo-electro-magnetic layers such as BaTiO₃ and CoFe₂O₄ that using these layer, one can be controlled the displacement

of sandwich plate that this idea can be stated in the future work. Thus, considering piezo-electro-magnetic layers as sensor and actuator can control the amplitude of vibration for a sandwich plate. Hence, by considering these investigations, many researches focused on GPLs reinforced composite, FG materials or the combination of piezoelectric materials with GPLs; thus we proposed an analytical solution on buckling behavior of sandwich plate with GPLs reinforced polymer-based composite integrated with piezoelectric face-sheets that is the novelty of this research. Regarding previous researches, this structure did not study in term of reinforcement effect on material properties improvements.

2. Geometric and fundamental formulation

A sandwich plate with FG-GPLs reinforced composite core with piezo-electro-magnetic facesheets is shown schematically in Fig. 1, in which a , b , h_c , h_p and H denote width, length, core thickness, piezo-electro-magnetic thickness and the total thickness of sandwich structure, respectively. It is noted that it must be defined $h=h_c/2$ in equations and Matlab codes.

The advantage of sandwich model in the present work is stated as follows.

By employing a sandwich model not only the total weight of a structure can be loss but the structure can be stiffened as well. In this work, a polymeric core has been considered to reduce the weight and stiff composite layers are applied to enhance the stiffness of the structure. In sandwich structures, researchers are looking to increase the strength to weight ratio.

The disadvantage of sandwich structure has been considered as

Making a coupling between these layers would be a serious issue in practice because in vibration discussion, the sandwich beam model is assumed to be as a continuous body that no delamination occurs between the layers of these sandwich structure. Thus if delamination is occurred, it is shown that in the manufacturing process, the layers do not couple as well as or under loadings, this phenomenon is occurred.

The limitations and assumptions of the present model have been stated as follows

(1) Making a coupling between these layers would be a serious issue in practice because in vibration discussion, the sandwich beam model is assumed to be as a continuous body that no delamination occurs between the layers of these sandwich structure.

(2) By employing a sandwich model not only the total weight of a structure can be loss but the structure can be stiffened as well. In this work, a porous core has been considered to reduce the weight and stiff composite layers are applied to enhance the stiffness of the structure. In sandwich structures, researchers are looking to increase the strength to weight ratio.

(3) The graphene platelets consider to increase the stiffness of a sandwich structure.

(4) The constitutive equations of this work are assumed linear in the elastic region.

(5) It assumed that the kinematic equations become linear.

2.1 Displacement fields

The displacement fields based on first-order shear deformation theory (FSDT) are obtained as follows

$$u(x, y, z, t) = u_0(x, y, t) + z\psi_x(x, y, t) \quad (1)$$

$$v(x, y, z, t) = v_0(x, y, t) + z\psi_y(x, y, t)$$

$$w(x, y, z, t) = w_0(x, y, t)$$

where, $u_0(x, y, t)$, $v_0(x, y, t)$ and $w_0(x, y, t)$ show mid-plane axially displacement, and $\psi_x(x, y, t)$ and $\psi_y(x, y, t)$ denote the rotations of mid-plane's normal about y and x axes, respectively.

The kinematic equations for each layer is expressed as follows

$$\begin{aligned}\varepsilon_{xx} &= u_{0,x}(x, y, t) + z\psi_{x,x}(x, y, t) \\ \varepsilon_{yy} &= u_{0,x}(x, y, t) + z\psi_{y,y}(x, y, t) \\ \gamma_{xy} &= u_{0,y}(x, y, t) + v_{0,x}(x, y, t) + z(\psi_{x,y}(x, y, t) + \psi_{y,x}(x, y, t)) \\ \gamma_{xz} &= \psi_x(x, y, t) + w_{0,x}(x, y, t) \\ \gamma_{yz} &= \psi_y(x, y, t) + w_{0,y}(x, y, t)\end{aligned}\quad (2)$$

2.2 Effective material properties of FG-GPLRC-The extend rule of mixture

In this sections we discuss the material properties of the core which is made of isotropic polymer as matrix and GPLs as reinforcement. The GPLs distribution can be random or uniform so we discuss four distributions patterns and the effect on buckling. Also weight fractions equation shows the FG effect on mechanical properties (Bahaadini and Saidi 2018)

$$U - GPLRPC : V_{GPL} = V_{GPL}^* \quad (3-a)$$

$$A - GPLRPC : V_{GPL} = V_{GPL}^* |2k - 1|/N_L \quad (3-a)$$

$$X - GPLRPC : V_{GPL} = 2V_{GPL}^* |2k - N_L - 1|/N_L \quad (3-a)$$

$$O - GPLRPC : V_{GPL} = 2V_{GPL}^* (1 - |2k - N_L - 1|/N_L) \quad (3-d)$$

where,

$$V_{GPL}^* = \frac{W_{GPL}}{W_{GPL} + (\rho_{GPL}/\rho_m)(1 - W_{GPL})} \quad (4)$$

In which $k=1,2,3,\dots, N_L$, ρ_{GPL} , ρ_m , and W_{GPL} are the mass density of graphene platelets (GPL), mass density of matrix and GPL weight fraction, respectively. Also, the subscripts "m" and "GPL" consider the matrix and GPL, respectively. The effective Young's modulus of GPLs reinforced composite obtained based on Halpin-Tsai micromechanics model as follows (Bahaadini and Saidi 2018)

$$E = \frac{3}{8} \frac{1 + \xi_L \eta_L V_{GPL}}{1 - \eta_L V_{GPL}} E_m + \frac{5}{8} \frac{1 + \xi_T \eta_T V_{GPL}}{1 - \eta_T V_{GPL}} E_m \quad (5)$$

where, ξ_L and ξ_T versus geometric parameters of GPL, and η_L and η_T versus geometric and material properties of GPL are defined as follows

$$\eta_L = \frac{(E_{GPL}/E_m) - 1}{(E_{GPL}/E_m) + \xi_L}, \quad \xi_L = 2 \frac{a_{GPL}}{t_{GPL}} \quad (6)$$

$$\eta_T = \frac{(E_{GPL}/E_m) - 1}{(E_{GPL}/E_m) + \xi_T}, \quad \xi_T = 2 \frac{b_{GPL}}{t_{GPL}}$$

The subscript “m” and “GPL” denotes properties of polymer matrix and GPL, respectively. Also, a_{GPL} , b_{GPL} and t_{GPL} shows the length, width and thickness of graphene platelets, respectively. The effective Poisson’s ratio and mass density achieved from rule of mixture.

$$\begin{aligned} \rho &= V_{GPL}\rho_{GPL} + V_m\rho_m \\ v &= V_{GPL}v_{GPL} + V_mv_m \end{aligned} \quad (7)$$

where v_{GPL} and v_m are Poisson’s ratio for GPL and matrix, respectively.

The polymer matrix volume fraction is V_m that is obtained as below

$$V_m = 1 - V_{GPL} \quad (8)$$

2.3 The constitutive equations for polymeric core

Stress-strain relations for FG-GPL reinforced composite expressed as below (Keleshteri *et al.* 2017)

$$\begin{Bmatrix} \sigma_{xx} \\ \sigma_{yy} \\ \tau_{yz} \\ \tau_{xz} \\ \tau_{xy} \end{Bmatrix} = \begin{bmatrix} c_{11} & c_{12} & 0 & 0 & 0 \\ c_{21} & c_{22} & 0 & 0 & 0 \\ 0 & 0 & c_{44} & 0 & 0 \\ 0 & 0 & 0 & c_{55} & 0 \\ 0 & 0 & 0 & 0 & c_{66} \end{bmatrix} \begin{Bmatrix} \varepsilon_{xx} \\ \varepsilon_{yy} \\ \gamma_{yz} \\ \gamma_{xz} \\ \gamma_{xy} \end{Bmatrix} \quad (9)$$

where, constants in stiffness matrix [C] are calculated as (Keleshteri *et al.* 2017)

$$\begin{aligned} &(c_{11}, c_{22}, c_{12}, c_{44}, c_{55}, c_{66}) \\ &= \left(\frac{E_{11}}{1 - \nu_{12}\nu_{21}}, \frac{E_{22}}{1 - \nu_{12}\nu_{21}}, \frac{\nu_{21}E_{11}}{1 - \nu_{12}\nu_{21}}, G_{23}, G_{13}, G_{12} \right) \end{aligned} \quad (10)$$

2.4 Piezo-electro-magnetic face-sheets

We assume that piezo-electro-magnetic face-sheets are homogenous, isotropic and polarized along the thickness, so the constitutive relations is defined as (Keleshteri *et al.* 2017)

$$\begin{Bmatrix} \sigma_{xx}^P \\ \sigma_{yy}^P \\ \tau_{yz}^P \\ \tau_{xz}^P \\ \tau_{xy}^P \end{Bmatrix} = \begin{bmatrix} c_{11}^E & c_{12}^E & 0 & 0 & 0 \\ c_{21}^E & c_{22}^E & 0 & 0 & 0 \\ 0 & 0 & c_{44}^E & 0 & 0 \\ 0 & 0 & 0 & c_{55}^E & 0 \\ 0 & 0 & 0 & 0 & \frac{(c_{11}^E - c_{12}^E)}{2} \end{bmatrix} \begin{Bmatrix} \varepsilon_{xx} \\ \varepsilon_{yy} \\ \gamma_{yz} \\ \gamma_{xz} \\ \gamma_{xy} \end{Bmatrix} - \begin{bmatrix} 0 & 0 & \bar{e}_{31} \\ 0 & 0 & \bar{e}_{32} \\ 0 & \bar{e}_{24} & 0 \\ \bar{e}_{15} & 0 & 0 \\ 0 & 0 & 0 \end{bmatrix} \quad (11)$$

$$\begin{Bmatrix} E_x \\ E_y \\ E_z \end{Bmatrix} = \begin{bmatrix} 0 & 0 & \bar{q}_{31} \\ 0 & 0 & \bar{q}_{32} \\ 0 & \bar{q}_{24} & 0 \\ \bar{q}_{15} & 0 & 0 \\ 0 & 0 & 0 \end{bmatrix} \begin{Bmatrix} H_x \\ H_y \\ H_z \end{Bmatrix}$$

where, E_x , E_y and E_z are the electric fields in the x, y, and z directions, respectively. H_x , H_y and H_z denote the magnetic fields in the x, y, and z directions, respectively. \bar{e}_{ij} and \bar{q}_{ij} are the piezoelectric and the piezomagnetic constants, respectively.

Also, the stiffness, piezoelectric and piezomagnetic constants are expressed as

$$\begin{aligned} (c_{11}^E, c_{22}^E, c_{12}^E, c_{44}^E, c_{55}^E) &= \left(\bar{c}_{11} - \frac{\bar{c}_{13}^2}{\bar{c}_{33}}, c_{11}^E, \bar{c}_{12} - \frac{\bar{c}_{13}^2}{\bar{c}_{33}} \right) \\ (\bar{e}_{31}, \bar{e}_{32}, \bar{e}_{15}, \bar{e}_{24}) &= (e_{31} - \frac{\bar{c}_{13}}{\bar{c}_{33}} e_{33}, \bar{e}_{31}, e_{15}, e_{24}) \\ (\bar{q}_{31}, \bar{q}_{32}, \bar{q}_{15}, \bar{q}_{24}) &= (q_{31} - \frac{\bar{c}_{13}}{\bar{c}_{33}} q_{33}, \bar{q}_{31}, q_{15}, q_{24}) \end{aligned} \quad (12)$$

Electric and magnetic displacement tensor is expressed as follows (Yazdani *et al.* 2019)

$$\begin{Bmatrix} D_x \\ D_y \\ D_z \end{Bmatrix} = \begin{bmatrix} 0 & 0 & 0 & \bar{e}_{15} & 0 \\ 0 & 0 & \bar{e}_{24} & 0 & 0 \\ \bar{e}_{31} & \bar{e}_{32} & 0 & 0 & 0 \end{bmatrix} \begin{Bmatrix} \varepsilon_{xx} \\ \varepsilon_{yy} \\ \gamma_{yx} \\ \gamma_{xz} \\ \gamma_{xy} \end{Bmatrix} + \begin{bmatrix} s_{11} & 0 & 0 \\ 0 & s_{22} & 0 \\ 0 & 0 & s_{33} \end{bmatrix} \begin{Bmatrix} E_x \\ E_y \\ E_z \end{Bmatrix} \\ + \begin{bmatrix} g_{11} & 0 & 0 \\ 0 & g_{21} & 0 \\ 0 & 0 & g_{33} \end{bmatrix} \begin{Bmatrix} H_x \\ H_y \\ H_z \end{Bmatrix} \quad (13)$$

$$\begin{Bmatrix} B_x \\ B_y \\ B_z \end{Bmatrix} = \begin{bmatrix} 0 & 0 & 0 & \bar{q}_{15} & 0 \\ 0 & 0 & q_{24} & 0 & 0 \\ \bar{q}_{31} & \bar{q}_{32} & 0 & 0 & 0 \end{bmatrix} \begin{Bmatrix} \varepsilon_{xx} \\ \varepsilon_{yy} \\ \gamma_{yx} \\ \gamma_{xz} \\ \gamma_{xy} \end{Bmatrix} + \begin{bmatrix} g_{11} & 0 & 0 \\ 0 & g_{22} & 0 \\ 0 & 0 & g_{33} \end{bmatrix} \begin{Bmatrix} E_x \\ E_y \\ E_z \end{Bmatrix} \\ + \begin{bmatrix} \mu_{11} & 0 & 0 \\ 0 & \mu_{21} & 0 \\ 0 & 0 & \mu_{33} \end{bmatrix} \begin{Bmatrix} H_x \\ H_y \\ H_z \end{Bmatrix} \quad (14)$$

where, D_x , D_y , and D_z are the electrical displacements and B_x , B_y , and B_z denote the magnetic displacements.

Also, s , g , and μ denote the dielectric, magneto-electric and magnetic constants that relations are as follows and electric and magnetic field are considered as

$$\begin{aligned} E_i &= -\phi_{,i}, H_i = -\Psi_{,i}; i = 1,2,3 \\ (s_{11}, s_{22}, s_{33}) &= \left(\bar{s}_{11}, \bar{s}_{22}, \bar{s}_{33} + \frac{e_{33}^2}{\bar{c}_{33}} \right) \end{aligned} \quad (15)$$

$$\begin{aligned}
 (g_{11}, g_{22}, g_{33}) &= \left(\bar{g}_{11}, \bar{g}_{22}, \bar{g}_{33} + \frac{q_{33}e_{33}}{\bar{c}_{33}} \right) \\
 (\mu_{11}, \mu_{22}, \mu_{33}) &= \left(\bar{\mu}_{11}, \bar{\mu}_{22}, \bar{\mu}_{33} + \frac{q_{33}^2}{\bar{c}_{33}} \right)
 \end{aligned}
 \tag{16}$$

In this paper, electric and magnetic potentials of the piezo-electromagnetic face-sheets are calculated as below to express the direct and transverse effect of material by applying external electric and magnetic fields (Keleshteri *et al.* 2017)

$$\phi = \left\{ \begin{aligned} &\phi(x, y) \sin\left(\frac{\pi(z - (h + h_p))}{h_p}\right) + \left(\frac{2z - (h_p + 2h)}{2h_p}\right) V_0 : h \leq z \leq h + h_p \\ &\phi(x, y) \sin\left(\frac{-\pi(z + (h + h_p))}{h_p}\right) + \left(\frac{2z + (h_p + 2h)}{2h_p}\right) V_0 : -(h + h_p) \leq z \leq -h \end{aligned} \right\} \tag{17}$$

$$\psi = \left\{ \begin{aligned} &\psi(x, y) \sin\left(\frac{\pi(z - (h + h_p))}{h_p}\right) + \left(\frac{2z - (h_p + 2h)}{2h_p}\right) \Psi_0 : h \leq z \leq h + h_p \\ &\psi(x, y) \sin\left(\frac{-\pi(z + (h + h_p))}{h_p}\right) + \left(\frac{2z + (h_p + 2h)}{2h_p}\right) \Psi_0 : -(h + h_p) \leq z \leq -h \end{aligned} \right\} \tag{18}$$

$$\text{TOP: } \phi(x, y, h) = -\frac{V_0}{2}; \phi(x, y, h + h_p) = \frac{V_0}{2} \tag{19}$$

$$\text{BOTTOM: } \phi(x, y, -h - h_p) = -\frac{V_0}{2}; \phi(x, y, -h) = \frac{V_0}{2}$$

where $\phi(x, y)$, and $\psi(x, y)$ are the electric and magnetic potentials, respectively.

It is noted that it must be defined $h=h_c/2$ in equations and Matlab codes.

3. The governing equations of motion

In this article, to obtain the governing equations of motion, the minimum total potential energy is employed.

$$\Pi = U + W_{ext}, \delta\Pi = 0 \rightarrow \delta U + \delta W_{ext} = 0 \tag{20}$$

where U and W_{ext} show the strain energy and external work, respectively.

The strain energy for the sandwich plate is considered as follows

$$\begin{aligned}
 U = \frac{1}{2} \int_V &[\sigma_{xx}\epsilon_{xx} + \sigma_{yy}\epsilon_{yy} + \sigma_{xy}\gamma_{xy} + k_s\sigma_{xz}\gamma_{xz} + k_s\sigma_{yz}\gamma_{yz} - D_x E_x - D_y E_y - D_z E_z \\ &- B_x H_x - B_y H_y - B_z H_z] dV
 \end{aligned} \tag{21-a}$$

$$\delta U = \oint_V [\sigma_{xx}\delta\varepsilon_{xx} + \sigma_{yy}\delta\varepsilon_{yy} + \sigma_{xy}\delta\gamma_{xy} + k_s\sigma_{xz}\delta\gamma_{xz} + k_s\sigma_{yz}\delta\gamma_{yz} - D_x\delta E_x - D_y\delta E_y - D_z\delta E_z - B_x\delta H_x - B_y\delta H_y - B_z\delta H_z] dV \quad (21-b)$$

where k_s is the shear correction factor.

The shear correction factor (k_s) must be considered for FSDT that in this research, the authors have been employed its, in this theory, the shear stress in the top and bottom structures becomes constant while the shear stress must be zero and in the mid plane, we have the maximum shear stress, thus the shear correction factor considers to improve the shear stress in the top and bottom sandwich structures.

The variation of the external work due to the biaxial buckling loads is defined as follows

$$\delta W_{ext} = - \int [N_{x_0} w_{0,xx} \delta w_0 + N_{y_0} w_{0,yy} \delta w_0 + N_{xy_0} w_{0,xy} \delta w_0] dA \quad (22)$$

Substituting Eqs. (21-b) and (22) into Eq. (20), we have

$$\begin{aligned} \delta \Pi = \oint_A [& (N_{x,x} + N_{xy,y}) \delta u_0 + (N_{y,y} + N_{xy,x}) \delta v_0 + N_{x_0} w_{0,xx} + N_{y_0} w_{0,yy} + 2N_{xy_0} w_{0,xy} \\ & + (k(N_{xz,x} + N_{yz,y})) \delta w_0 + (M_{x,x} + M_{xy,y} - k_s N_{xz}) \delta \psi_x \\ & + (M_{y,y} + M_{xy,x} - k_s N_{yz}) \delta \psi_y + (\int (D_{x,x} + D_{y,y} + D_{z,z}) dz) \delta \phi \\ & + (\int (B_{x,x} + B_{y,y} + B_{z,z}) dz) \delta \psi] dA \end{aligned} \quad (23)$$

The governing equations of equilibrium for sandwich plates with polymeric core and piezo-electro-magnetic fase-sheets based on Eq. (23) are obtained as follows

$$\begin{aligned} \delta u_0 : N_{x,x} + N_{xy,y} &= 0 \\ \delta v_0 : N_{y,y} + N_{xy,x} &= 0 \\ \delta w_0 : + N_{x_0} w_{0,xx} + N_{y_0} w_{0,yy} + 2N_{xy_0} w_{0,xy} + k_s(Q_{x,x} + Q_{y,y}) &= 0 \\ \delta \psi_x : M_{x,x} + M_{xy,y} - k_s Q_x &= 0 \\ \delta \psi_y : M_{y,y} + M_{xy,x} - k_s Q_y &= 0 \\ \delta \phi : \int (D_{x,x} + D_{y,y} + D_{z,z}) dz &= 0 \\ \delta \Psi : \int (B_{x,x} + B_{y,y} + B_{z,z}) dz &= 0 \end{aligned} \quad (24)$$

where the resultants forces and moments have been defined as follows

$$(N_x, N_y, N_{xy}) = \int_{-h}^h (\sigma_{xx}, \sigma_{yy}, \tau_{xy}) dz + \int_{-(h+h_p)}^{-h} (\sigma_{xx}^p, \sigma_{yy}^p, \tau_{xy}^p) dz$$

$$\begin{aligned}
 & + \int_h^{h+h_p} (\sigma_{xx}^p, \sigma_{yy}^p, \tau_{xy}^p) dz (M_x, M_y, M_{xy}) \\
 & = \int_{-h}^h z(\sigma_{xx}, \sigma_{yy}, \tau_{xy}) dz + \int_{-(h+h_p)}^{-h} z(\sigma_{xx}^p, \sigma_{yy}^p, \tau_{xy}^p) dz \\
 & + \int_h^{h+h_p} z(\sigma_{xx}^p, \sigma_{yy}^p, \tau_{xy}^p) dz
 \end{aligned} \tag{25}$$

$$(Q_x, Q_y) = \int_{-h}^h (\tau_{xz}, \tau_{yz}) dz + \int_{-(h+h_p)}^{-h} (\tau_{xz}^p, \tau_{yz}^p) dz + \int_h^{h+h_p} (\tau_{xz}^p, \tau_{yz}^p) dz$$

It is noted that it must be defined $h=h_c/2$ in above equations.

4. Solution procedure

In this research, the analytical method for sandwich structure with polymeric core and piezo-electro-magnetic face-sheets is used based on the Navier’s type solution as follows

$$\begin{aligned}
 u_0(x, y) &= \sum \sum u_{0mn} \cos\left(\frac{m\pi x}{a}\right) \sin\left(\frac{n\pi y}{b}\right) \\
 v_0(x, y) &= \sum \sum v_{0mn} \sin\left(\frac{m\pi x}{a}\right) \cos\left(\frac{n\pi y}{b}\right) \\
 \omega_0(x, y) &= \sum \sum \omega_{0mn} \sin\left(\frac{m\pi x}{a}\right) \sin\left(\frac{n\pi y}{b}\right) \\
 \psi_x(x, y) &= \sum \sum \psi_{x0mn} \cos\left(\frac{m\pi x}{a}\right) \sin\left(\frac{n\pi y}{b}\right) \\
 \psi_y(x, y) &= \sum \sum \psi_{y0mn} \sin\left(\frac{m\pi x}{a}\right) \cos\left(\frac{n\pi y}{b}\right) \\
 \phi(x, y) &= \sum \sum \phi_{0mn} \sin\left(\frac{m\pi x}{a}\right) \sin\left(\frac{n\pi y}{b}\right) \\
 \Psi(x, y) &= \sum \sum \Psi_{0mn} \sin\left(\frac{m\pi x}{a}\right) \sin\left(\frac{n\pi y}{b}\right)
 \end{aligned} \tag{26}$$

By substituting the Eqs. (9), (11), (13), and (14) into the equations (25), the resultants forces and moments versus the displacements have been obtained, then this results have been placed into Eq. (24), thus the governing equations of equilibrium for a sandwich plate with polymeric core integrated with piezo-electro-magnetic layers reinforced by graphene platelets are derived. Finally, by substituting Eq. (26) into the obtained governing equations of equilibrium, the buckling and stiffness matrices have been obtained.

5. Numerical results and discussion

In this section, we study the effect of different parameters such as GPLs thickness and width of graphene platelets. Also, the effect of electric and magnetic fields are investigated on critical

Table 1 the geometric and material properties for face sheets and core layers

Geometric	Core	Face sheets layer
$H = 2.4\text{mm}$, $h_c = 0.5H$, $h_g = 0.2H$, $h_p = 0.05H$, $a = b = 10H$, $k_s = 5/6$.	$E_c = 3\text{GPa}$, $\rho_c = 1200\text{kg/m}^3$, $\nu_c = 0.34$	$E_m = 2.5\text{GPa}$, $\rho_m = 1150\text{kg/m}^3$, $\nu_m = 0.33$, $E_{GNP} = 1.01\text{TPa}$, $\nu_{GNP} = 0.186$, $\rho_{GNP} = 1062.5\text{kg/m}^3$, $w_{GNP} = 0.2\%$

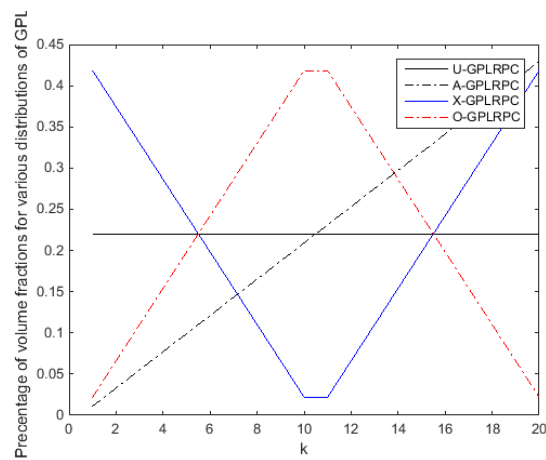


Fig. 2 The effect of percentage of volume fraction for various distributions of GPL

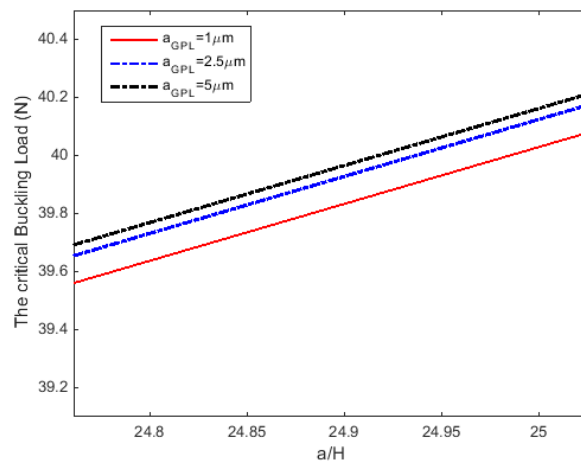


Fig. 3 The effect of GPLs length on the critical biaxial buckling load of piezo-electro-magnetic reinforced polymeric core

buckling load versus plate's width to total thickness of the sandwich plate.

Table 1 shows the geometric and material properties for face sheets and core layers from this research. It is known that the range thickness of core is 0.4 H to 0.9 H, also the range for each

facesheet layers becomes $0.05H$ to $0.3H$, and the range for each piezo-electro-magnetic layers becomes $0.05H$ to $0.1H$, thus, we consider the parameters according to Table 1. It is noted that the researcher follow the higher stiffness and lower weight. Moreover, the authors employed the GPL as reinforcement to increase the stiffness of a sandwich plate. Also, they used polymeric core to decrease the weight of these structure, because in mechanical science, the researcher follow to increase the high strength to weight.

Fig. 2 shows the effect of percentage of volume fraction for various distributions of GPL including U, A, X, and O-GPLRPC. It is seen that in top and bottom layers and the farthest distance from the neutral axes for the X pattern is more than the others. Thus in this case, the stiffness of a sandwich structure is more than the other cases.

Fig. 3 shows the effect of GPL length on the critical biaxial buckling load. It can be seen that with increasing the length of GPL, the critical buckling load increases because the stiffness of the structures enhances.

Fig. 4 presents different N_x/N_y ratios effect on critical buckling for a sandwich plate with polymeric core integrated with piezo-electro-magnetic layers reinforced by graphene platelets. It is concluded from investigating three different ratios such as 0, 0.5 and 1 that $N_x/N_y=1$ has the lowest critical buckling load so by increasing this ratio, the critical buckling load decreases. On the other hands, the biaxial critical buckling load is lower that of uniaxial buckling load because the sandwich structure is under compressive forces from two directions.

The effect of core thickness to total thickness ratio on the critical biaxial buckling load are plotted in Fig. 5. It is shown from this figure that increasing this ratio leads to decrease the critical buckling load. On the other hands, the sandwich plate becomes softer. By employing a sandwich model not only the total weight of a structure can be loss but the structure can be stiffened as well. In this work, a porous core has been considered to reduce the weight and stiff composite layers are applied to enhance the stiffness of the structure. In sandwich structures, researchers are looking to increase the strength to weight ratio.

Fig. 6(a) illustrates the effect of different material properties including the electric properties (BaTiO₃) and magnetic properties (CoFe₂O₄) on the critical buckling load versus non-dimensional plate. Also, in Fig. 6(b), it is seen that if the effect of piezo-electro-magnetic loadings

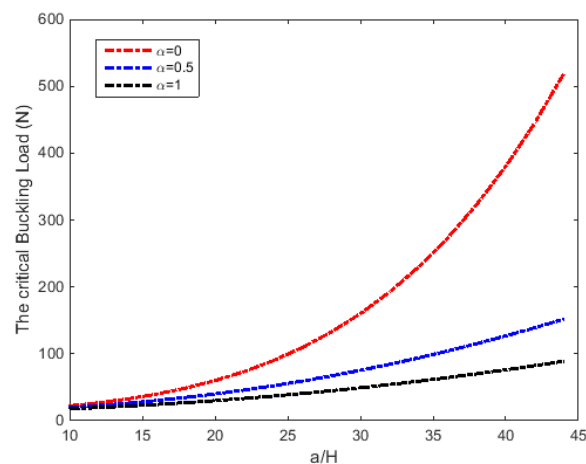


Fig. 4 The effect of different α (N_x/N_y) on the critical buckling load of a sandwich plate with polymeric core integrated with piezo-electro-magnetic layers reinforced by graphene platelets

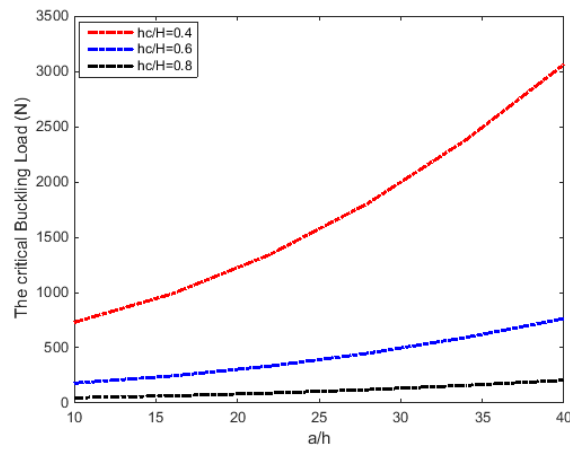


Fig. 5 The effect of different hc/h ratio on biaxial critical buckling load for different values of a/h

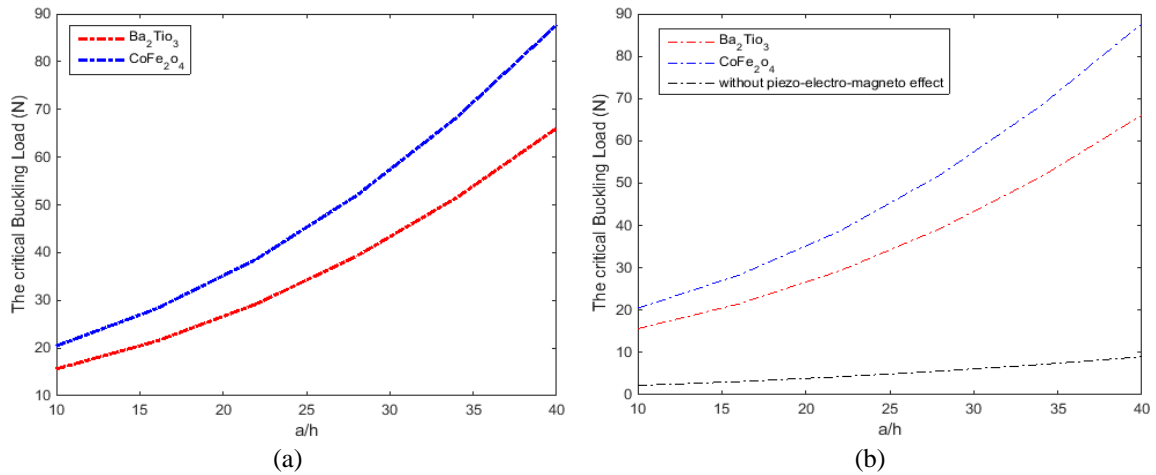


Fig. 6 Biaxial critical buckling load versus non-dimensional plate length for (a) Two different material properties (b) Without considering piezo-electro-magneto effect

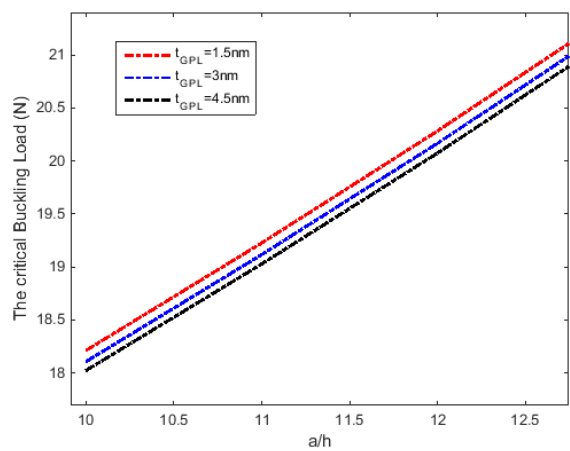


Fig. 7 Critical biaxial buckling load for different GPLs thickness versus non-dimensional plate length

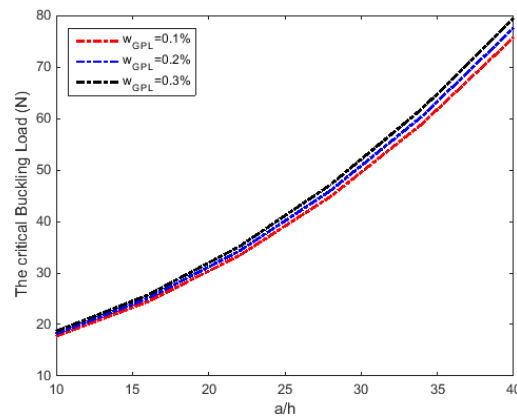


Fig. 8 Critical biaxial buckling load for different GPLs weight fraction versus non-dimensional plate length

on the critical buckling load is ignored, the critical buckling load is lower than considering the electric and magnetic properties because with the presence piezo-electro-magneto layers, the stiffness of a sandwich structures increases. It is seen that the critical buckling load for the electric properties (BaTiO₃) are lower than magnetic properties (CoFe₂O₄).

In Figs. 7 and 8 investigated effect of thickness and weight fraction of GPLs, respectively. It is shown that by increasing GPLs thickness, the critical biaxial buckling load decreases according to the Fig. 7 because the structure becomes softer. Also, it can be seen that increasing weight fraction leads to increase in critical biaxial buckling load are shown in Fig. 8, because of the stiffness of sandwich plate increases.

6. Conclusions

In this article, an analytical study on buckling behavior of a sandwich plate with polymeric core integrated with piezo-electro-magnetic layers reinforced by graphene platelets (GPLs) is investigated. The Halpin-Tsai micromechanics model is used to describe the properties of the graphene platelets. The governing equations of equilibrium are obtained from first-order shear deformation theory (FSDT) and the Navier's method is employed to solve the equations. The results showed the effect different parameters such as thickness ratio, length, weight fraction of GPLs, two different materials used in core structure such as BaTiO₃ and CoFe₂O₄ and also the effect of electric and magnetic field on critical buckling load.

The main results of this study presented as follows

- The influence of different N_x/N_y shows that increasing this ratio decreases critical buckling load. On the other hands, the biaxial critical buckling load is lower that of uniaxial buckling load.
- It is shown from this figure that increasing this ratio leads to decrease the critical buckling load. On the other hands, the sandwich plate becomes softer.
- It is seen that the critical buckling load for the electric properties (BaTiO₃) are lower than magnetic properties (CoFe₂O₄).
- It is shown that by increasing GPLs thickness, the critical biaxial buckling load decreases.
- It can be seen that increasing weight fraction leads to increase in critical biaxial buckling load,

because of the stiffness of sandwich plate increases.

The result of this study can be obtained in the aerospace industry and also in the design of sensors and actuators and some further analysis on the use of piezo-electro-magnetic material as active control in the bending, free vibration or buckling problems.

Acknowledgment

The authors would like to thank the reviewers for their valuable comments and suggestions to improve the clarity of this work. Also, they would like to thank the Iranian Nanotechnology Development Committee for their financial support and the University of Kashan for supporting this work by Grant No. 891238/22.

References

- Anitescu, C., Atroshchenko, E., Alajlan, N. and Rabczuk, T. (2019), "Artificial neural network methods for the solution of second order boundary value problems", *Comput. Mater. Contin.*, **59**(1), 345-359. <https://doi.org/10.32604/cmc.2019.06641>.
- Arani, A.G., Maghamikia, S., Mohammadimehr, M. and Arefmanesh, A. (2011a), "Buckling analysis of laminated composite rectangular plates reinforced by SWCNTs using analytical and finite element methods", *J. Mech. Sci. Technol.*, **25**(3), 809-820. <https://doi.org/10.1007/s12206-011-0127-3>.
- Arefi, M., Mohammad-Rezaei Bidgoli, E., Dimitri, R., Baccocchi, M. and Tornabene, F. (2019), "Nonlocal bending analysis of curved nanobeams reinforced by graphene nanoplatelets", *Compos. B. Eng.*, **166**, 1-12. <https://doi.org/10.1016/j.compositesb.2018.11.092>.
- Bahaadini, R. and Saidi, A.R. (2018), "Aeroelastic analysis of functionally graded rotating blades reinforced with graphene nanoplatelets in supersonic flow", *Aerosp. Sci. Technol.*, **80**, 381-391. <https://doi.org/10.1016/j.ast.2018.06.035>.
- Bamdad, M., Mohammadimehr, M. and Alambeigi, K. (2019), "Analysis of sandwich Timoshenko porous beam with temperature-dependent material properties: Magneto-electro-elastic vibration and buckling solution", *J. Vib. Control*, **25**(23-24), 2875-2893. <https://doi.org/10.1177/1077546319860314>.
- Canbay, C.A., Karaduman, O., Ibrahim, P.A. and Özkul, I. (2021), "Thermostructural shape memory effect observations of ductile Cu-Al-Mn smart alloy", *Adv. Mater. Res.*, **10**(1), 45-56. <https://doi.org/10.12989/amr.2021.10.1.045>.
- Chan, D.Q., Van Thanh, N., Khoa, N.D. and Duc, N.D. (2020), "Nonlinear dynamic analysis of piezoelectric functionally graded porous truncated conical panel in thermal environments", *Thin Wall. Struct.*, **154**, 106837. <https://doi.org/10.1016/j.tws.2020.106837>.
- Cong, P.H. and Duc, N.D. (2016), "Vibration and nonlinear dynamic analysis of imperfect thin eccentrically stiffened functionally graded plates in thermal environments", *VNU J. Math. Phys.*, **32**(1), 1-19.
- Dat, N.D., Quan, T.Q., Mahesh, V. and Duc, N.D. (2020), "Analytical solutions for nonlinear magneto-electro-elastic vibration of smart sandwich plate with carbon nanotube reinforced nanocomposite core in hygrothermal environment", *Int. J. Mech. Sci.*, **186**, 105906. <https://doi.org/10.1016/j.ijmecsci.2020.105906>.
- Di Sciuva, M. and Sorrenti, M. (2019), "Bending, free vibration and buckling of functionally graded carbon nanotube-reinforced sandwich plates, using the extended Refined Zigzag Theory", *Compos. Struct.*, **227**, 111324. <https://doi.org/10.1016/j.compstruct.2019.111324>.
- Vuong, P.M. and Duc, N.D. (2020), "Nonlinear static and dynamic stability of functionally graded toroidal shell segments under axial compression", *Thin Wall. Struct.*, **155**, 106973. <https://doi.org/10.1016/j.tws.2020.106973>.

- Duc, N.D. (2016), "Nonlinear thermal dynamic analysis of eccentrically stiffened S-FGM circular cylindrical shells surrounded on elastic foundations using the Reddy's third-order shear deformation shell theory", *Eur. J. Mech. A/Solid.*, **58**, 10-30. <https://doi.org/10.1016/j.euromechsol.2016.01.004>.
- Duc, N.D. (2016), "Nonlinear thermo-electro-mechanical dynamic response of shear deformable piezoelectric sigmoid functionally graded sandwich circular cylindrical shells on elastic foundations", *J. Sandw. Struct. Mater.*, **20**(3), 351-378. <https://doi.org/10.1177/1099636216653266>.
- Duc, N.D., Quan, T.Q. and Cong, P.H. (2021), "Nonlinear vibration of auxetic plates and shells".
- Duc, N.D., Van Tung, H. (2010), "Nonlinear analysis of stability for functionally graded cylindrical panels under axial compression", *Comput. Mater. Sci.*, **49**(4), S313-S316. <https://doi.org/10.1016/j.commatsci.2009.12.030>.
- Duc, N.D., Thang, P.T., Dao, N.T. and Tac, H.V. (2015), "Nonlinear buckling of higher deformable S-FGM thick circular cylindrical shells with metal-ceramic-metal layers surrounded on elastic foundations in thermal environment", *J. Compos. Struct.*, **121**, 134-141. <https://doi.org/10.1016/j.compstruct.2014.11.009>.
- Duc, N.D., Tuan, N.D., Tran, P., Cong, P.H. and Nguyen, P.D. (2016), "Nonlinear stability of eccentrically stiffened S-FGM elliptical cylindrical shells in thermal environment", *Thin Wall. Struct.*, **108**, 280-290. <https://doi.org/10.1016/j.tws.2016.08.025>.
- Draiche, K., Bousahla, A.A., Tounsi, A., Alwabli, A.S. and Mahmoud, S.R. (2019), "Static analysis of laminated reinforced composite plates using a simple first-order shear deformation theory", *Comput. Concrete*, **24**(4), 369-378. <https://doi.org/10.12989/cac.2019.24.4.369>.
- García-Macías, E., Rodríguez-Tembleque, L. and Sáez, A. (2018), "Bending and free vibration analysis of functionally graded graphene vs. carbon nanotube reinforced composite plates", *Compos. Struct.*, **186**, 123-138. <https://doi.org/10.1016/j.compstruct.2017.11.076>.
- Ghadiri, M. and S Hosseini, S.H. (2021), "Nonlinear forced vibration of graphene/piezoelectric sandwich nanoplates subjected to a mechanical shock", *J. Sandw. Struct. Mater.*, **23**(3), 956-987. <https://doi.org/10.1177/1099636219849647>.
- Ghorbanpourarani, A., Navi, B.R., Mohammadimehr, M. and Niknejad, S. (2019), "Pull-in instability of MSGT piezoelectric polymeric FG-SWCNTs reinforced nanocomposite considering surface stress effect", *J. Solid Mech.*, **11**(4), 759-777. <https://doi.org/10.22034/jsm.2019.668611>.
- Guo, H., Zhuang, X. and Rabczuk, T. (2019), "A deep collocation method for the bending analysis of kirchhoff plate", *Comput. Mater. Contin.*, **59**(2), 433-456. <https://doi.org/10.32604/cmc.2019.06660>.
- Hadji, L. and Bernard, F. (2020), "Bending and free vibration analysis of functionally graded beams on elastic foundations with analytical validation", *Adv. Mater. Res.*, **9**(1), 63-98. <https://doi.org/10.12989/amr.2020.9.1.063>.
- Jia, J., Zhao, J., Xu, G., Di, J., Yong, Z., Tao, Y. and Li, Q. (2011), "A comparison of the mechanical properties of fibers spun from different carbon nanotubes", *Carbon*, **49**(4), 1333-1339. <https://doi.org/10.1016/j.carbon.2010.11.054>.
- Karimiasl, M., Ebrahimi, F. and Mahesh, V. (2020), "On nonlinear vibration of sandwiched polymer-CNT/GPL-fiber nanocomposite nanoshells", *Thin Wall. Struct.*, **146**, 106431. <https://doi.org/10.1016/j.tws.2019.106431>.
- Keleshteri, M.M., Asadi, H. and Wang, Q. (2017), "On the snap-through instability of post-buckled FG-CNTRC rectangular plates with integrated piezoelectric layers", *Comput. Meth. Appl. Mech. Eng.*, <https://doi.org/10.1016/j.cma.2017.11.015>.
- Khoa, N.D., Thiem, H.T. and Duc, N.D. (2019), "Nonlinear buckling and postbuckling of imperfect piezoelectric S-FGM circular cylindrical shells with metal-ceramic-metal layers in thermal environment using Reddy's third-order shear deformation shell theory", *Mech. Adv. Mater. Struct.*, **26**(3), 248-259. <https://doi.org/10.1080/15376494.2017.1341583>.
- Li, Z., Zheng, J. and Zhang, Z. (2019), "Mechanics of the confined functionally graded porous arch reinforced by graphene platelets", *Eng. Struct.*, **201**, 109817. <https://doi.org/10.1016/j.engstruct.2019.109817>.
- Mao, J.J. and Zhang, W. (2019), "Buckling and post-buckling analyses of functionally graded graphene reinforced piezoelectric plate subjected to electric potential and axial forces", *Compos. Struct.*, **216**, 392-405. <https://doi.org/10.1016/j.compstruct.2019.02.095>.

- Mohammadimehr, M. and Shahedi, S. (2016), "Nonlinear magneto-electro-mechanical vibration analysis of double-bonded sandwich Timoshenko microbeams based on MSGT using GDQM", *Steel Compos. Struct.*, **21**(1), 1-36. <https://doi.org/10.12989/scs.2016.21.1.001>.
- Mohammadimehr, M., Rostami, R. and Arefi, M. (2016), "Electro-elastic analysis of a sandwich thick plate considering FG core and composite piezoelectric layers on Pasternak foundation using TSDT", *Steel Compos. Struct.*, **20**(3), 513-544. <https://doi.org/10.12989/scs.2016.20.3.513>.
- Mohammadimehr, M., Shahedi, S. and Roustavi Navi, B. (2017), "Nonlinear vibration analysis of FG-CNTRC sandwich Timoshenko beam based on modified couple stress theory subjected to longitudinal magnetic field using generalized differential quadrature method", *Pro. Inst. Mech. Eng., Part C: J. Mech. Eng. Sci.*, **231**(20), 3866-3885. <https://doi.org/10.1177/0954406216653622>.
- Mousavi, M., Mohammadimehr, M. and Rostami, R. (2019), "Analytical solution for buckling analysis of micro sandwich hollow circular plate", *Comput. Concrete*, **24**(3), 185-192. <https://doi.org/10.12989/cac.2019.24.3.185>.
- Namayandeh, M.J., Mohammadimehr, M., Mehrabi, M. and Sadeghzadeh-Attar, A. (2020), "Temperature and thermal stress distributions in a hollow circular cylinder composed of anisotropic and isotropic materials", *Adv. Mater. Res.*, **9**(1), 15-32. <https://doi.org/10.12989/amr.2020.9.1.015>.
- Pashmforoush, F. (2019), "Statistical analysis on free vibration behavior of functionally graded nanocomposite plates reinforced by graphene platelets", *Compos. Struct.*, **213**, 14-24. <https://doi.org/10.1016/j.compstruct.2019.01.066>.
- Quan, T.Q., Van Quyen, N. and Duc, N.D. (2021), "An analytical approach for nonlinear thermo-electro-elastic forced vibration of piezoelectric penta-Graphene plates", *Eur. J. Mech. A/Solid.*, **85**, 104095. <https://doi.org/10.1016/j.euromechsol.2020.104095>.
- Reza, M. and Hossein, B. (2020), "Finite element forced vibration analysis of refined shear deformable nanocomposite graphene platelet-reinforced beams", *J. Braz. Soc. Mech. Sci. Eng.*, **8**, 1-14. <https://doi.org/10.1007/s40430-019-2118-8>.
- Rajabi, J. and Mohammadimehr, M. (2019), "Bending analysis of a micro sandwich skew plate using extended Kantorovich method based on Eshelby-Mori-Tanaka approach", *Comput. Concrete*, **23**(5), 361-376. <https://doi.org/10.12989/cac.2019.23.5.361>.
- Selim, B.A., Liu, Z. and Liew, K.M. (2019), "Active vibration control of functionally graded graphene nanoplatelets reinforced composite plates integrated with piezoelectric layers", *Thin Wall. Struct.*, **145**, 106372. <https://doi.org/10.1016/j.tws.2019.106372>.
- Song, M., Kitipornchai, S. and Yang, J. (2017), "Free and forced vibrations of functionally graded polymer composite plates reinforced with graphene nanoplatelets", *Compos. Struct.*, **159**, 579-588. <https://doi.org/10.1016/j.compstruct.2016.09.070>.
- Song, M., Yang, J. and Kitipornchai, S. (2018), "Bending and buckling analyses of functionally graded polymer composite plates reinforced with graphene nanoplatelets", *Compos. B. Eng.*, **134**, 106-113. <https://doi.org/10.1016/j.compositesb.2017.09.043>.
- Song, M., Yang, J., Kitipornchai, S. and Zhu, W. (2017), "Buckling and postbuckling of biaxially compressed functionally graded multilayer graphene nanoplatelet-reinforced polymer composite plates", *Int. J. Mech. Sci.*, **131**, 345-355. <https://doi.org/10.1016/j.ijmecsci.2017.07.017>.
- Sun, C.H., Li, F., Cheng, H.M. and Lu, G.Q. (2005), "Axial Young's modulus prediction of single-walled carbon nanotube arrays with diameters from nanometer to meter scales", *Appl. Phys. Lett.*, **87**(19), 1-3. <https://doi.org/10.1063/1.2119409>.
- Thai, C.H., Ferreira, A.J.M., Phung-van, P., Mechanics, C., Duc, T., Chi, H. and Nam, V. (2019), "Size dependent free vibration analysis of multilayer functionally graded GPLRC microplates based on modified strain gradient theory", *Compos. B. Eng.*, **169**, 174-188. <https://doi.org/10.1016/j.compositesb.2019.02.048>.
- Thai, C.H., Ferreira, A.J.M., Tran, T.D. and Phung-van, P. (2019), "Free vibration, buckling and bending analyses of multilayer functionally graded graphene nanoplatelets reinforced composite plates using the NURBS", *Compos. Struct.*, **220**, 749-759. <https://doi.org/10.1016/j.compstruct.2019.03.100>.
- Taherifar, R., Mahmoudi, M., Nasr Esfahani, M.H., Ashrafi Khuzani, N., Nasr Esfahani, S. and Chinaei, F. (2019), "Buckling analysis of concrete plates reinforced by piezoelectric nanoparticles", *Comput. Concrete*,

- 23(4), 295-301. <https://doi.org/10.12989/cac.2019.23.4.295>.
- Wang, Y., Feng, C., Santiuste, C., Zhao, Z. and Yang, J. (2019), "Buckling and postbuckling of dielectric composite beam reinforced with graphene platelets (GPLs)", *Aerosp. Sci. Technol.*, **91**, 208-218. <https://doi.org/10.1016/j.ast.2019.05.008>.
- Yang, J., Chen, D. and Kitipornchai, S. (2018), "Buckling and free vibration analyses of functionally graded graphene reinforced porous nanocomposite plates based on Chebyshev-Ritz method", *Compos. Struct.*, **193**, 281-294. <https://doi.org/10.1016/j.compstruct.2018.03.090>.
- Yang, Z., Liu, A., Yang, J., Fu, J. and Yang, B. (2020), "Dynamic buckling of functionally graded graphene nanoplatelets reinforced composite shallow arches under a step central point load", *J. Sound Vib.*, **465**, 115019. <https://doi.org/10.1016/j.jsv.2019.115019>.
- Yazdani, R., Mohammadimehr, M. and Navi, B.R. (2019), "Free vibration of Cooper-Naghdi micro saturated porous sandwich cylindrical shells with reinforced CNT face sheets under magneto-hydro-thermo-mechanical loadings", *Struct. Eng. Mech.*, **70**(3), 351-365. <https://doi.org/10.12989/sem.2019.70.3.351>.
- Zhao, S., Yang, Z., Kitipornchai, S. and Yang, J. (2020), "Dynamic instability of functionally graded porous arches reinforced by graphene platelets", *Thin Wall. Struct.*, **147**, 106491. <https://doi.org/10.1016/j.tws.2019.106491>.
- Rahi, M.J., Rahmani Firoozjaee, A. and Dehestani, M. (2021), "Simplified numerical method for nonlocal static and dynamic analysis of a graphene nanoplate", *Adv. Mater. Res.*, **10**(1), 1-22. <https://doi.org/10.12989/amr.2021.10.1.001>.
- Rabia, B., Daouadji, T.H. and Abderezak, R. (2021), "Predictions of the maximum plate end stresses of imperfect FRP strengthened RC beams: Study and analysis", *Adv. Mater. Res.*, **9**(4), 265-287. <https://doi.org/10.12989/amr.2020.9.4.265>.
- Rabczuk, T., Ren, H. and Zhuang, X. (2019), "A nonlocal operator method for partial differential equations with application to electromagnetic waveguide problem", *Comput. Mater. Contin.*, **59**(1), 345-359. <https://doi.org/10.32604/cmc.2019.04567>.
- Samaniego, E., Anitescu, C., Goswami, S., Nguyen-Thanh, V.M., Guo, H., Hamdia, K., Zhuang, X. and Rabczuk, T. (2020), "An energy approach to the solution of partial differential equations in computational mechanics via machine learning: Concepts, implementation and applications", *Comput. Methods Appl. Mech. Eng.*, **362**, 112790. <https://doi.org/10.1016/j.cma.2019.112790>.
- Thang, P.T., Duc, N.D. and Trung, N.T. (2017), "Thermomechanical buckling and post-buckling of cylindrical shell with functionally graded coatings and reinforced by stringers", *Aerosp. Sci. Technol.*, **66**, 392-401. <https://doi.org/10.1016/j.ast.2017.03.023>.
- Yang, Z., Feng, C., Yang, J., Wang, Y., Lv, J., Liu, A. and Fu, J. (2020), "Geometrically nonlinear buckling of graphene platelets reinforced dielectric composite (GPLRDC) arches with rotational end restraints", *Aerosp. Sci. Technol.*, **107**, 106326. <https://doi.org/10.1016/j.ast.2020.106326>.
- Yang, Z., Liu, A., Lai, S.K., Safaei, B., Lv, J., Huang, Y. and Fu, J. (2022), "Thermally induced instability on asymmetric buckling analysis of pinned-fixed FG-GPLRC arches", *Eng. Struct.*, **250**, 113243. <https://doi.org/10.1016/j.engstruct.2021.113243>.
- Yang, Z., Wu, D., Yang, J., Lai, S.K., Lv, J., Liu, A. and Fu, J. (2021a), "Dynamic buckling of rotationally restrained FG porous arches reinforced with graphene nanoplatelets under a uniform step load", *Thin Wall. Struct.*, **166**, 108103. <https://doi.org/10.1016/j.tws.2021.108103>.
- Yang, Z., Lu, H., Sahmani, S. and Safaei, B. (2021b), "Isogeometric couple stress continuum-based linear and nonlinear flexural responses of functionally graded composite microplates with variable thickness", *Arch. Civil Mech. Eng.*, **21**, 114. <https://doi.org/10.1007/s43452-021-00264-w>.
- Tam, M., Yang, Z., Zhao, S., Zhang, H., Zhang, Y. and Yang, J. (2020), "Nonlinear bending of elastically restrained functionally graded graphene nanoplatelet reinforced beams with an open edge crack", *Thin Wall. Struct.*, **156**, 106972. <https://doi.org/10.1016/j.tws.2020.106972>.